Free Radical Research, July 2009; 43(7): 631–645

informa
healthcare

Effects of a metalloporphyrinic peroxynitrite decomposition catalyst, ww-85, in a mouse model of spinal cord injury

TIZIANA GENOVESE[1], EMANUELA MAZZON[1], EMANUELA ESPOSITO[1], ROSANNA DI PAOLA[1], KANNEGANTI MURTHY[2], LEWIS NEVILLE[2], PLACIDO BRAMANTI[1], & SALVATORE CUZZOCREA[1,3]

[1]*IRCCS Centro Neurolesi 'Bonino-Pulejo', Messina, Italy,* [2]*Inotek Pharmaceuticals Corporation Beverly, USA, and* [3]*Department of Clinical and Experimental Medicine and Pharmacology, School of Medicine, University of Messina, Italy*

(Received 8 January 2009; revised 3 April 2009)

Abstract

The aim of the present study was to assess the effect of a metalloporphyrinic peroxynitrite decomposition catalyst, ww-85, in the pathophysiology of spinal cord injury (SCI) in mice. Spinal cord trauma was induced by the application of vascular clips to the dura via a four-level T5–T8 laminectomy. SCI in mice resulted in severe trauma characterized by oedema, neutrophil infiltration, production of inflammatory mediators, tissue damage and apoptosis. ww-85 treatment (30–300 μg/kg, i.p. 1 h after the SCI) significantly reduced in a dose-dependent manner: (1) the degree of spinal cord inflammation and tissue injury, (2) neutrophil infiltration (myeloperoxidase activity), (3) nitrotyrosine formation and PARP activation, (4) pro-inflammatory cytokines expression, (5) NF-κB activation and (6) apoptosis. Moreover, ww-85 significantly ameliorated the recovery of limb function (evaluated by motor recovery score) in a dose-dependent manner. The results demonstrate that ww-85 treatment reduces the development of inflammation and tissue injury associated with spinal cord trauma.

Keywords: *Spinal cord injury, ww-85, peroxynitrite*

Introduction

An excessive post-traumatic inflammatory reaction may play an important role in the secondary injury processes, which develop after spinal cord injury (SCI) [1]. The primary traumatic mechanical injury to the spinal cord causes the death of a number of neurons that to date can neither be recovered nor regenerated. However, neurons continue to die for hours after SCI and this represents a potentially avoidable event [2]. This secondary neuronal death is determined by a large number of cellular, molecular and biochemical cascades. One such cascade that has been proposed to contribute significantly to the evolution of the secondary damage is the local inflammatory response in the injured spinal cord. While the precise mechanisms responsible remain undefined, several studies have implicated peroxynitrite ($ONOO^-$), a cytotoxic molecule generated when nitric oxide (NO) and superoxide ($O_2^{\cdot-}$) combine, in the secondary neuronal damage of SCI [3–11]. Not only $ONOO^-$ was detected in spinal cord tissues from rats following traumatic injury [7,8,10,11], but $ONOO^-$-donor administration directly into the rat spinal cord has been shown to cause neuronal cell death and neurological deficits [3–5]. Previous reports have demonstrated that $ONOO^-$ is toxic for neurons *in vitro* [12] and recently it have been also established that primary spinal cord neurons also undergo cell death following $ONOO^-$ treatment [9]. $ONOO^-$ is known to mediate several potentially destructive chemical reactions, including tyrosine nitration and lipid peroxidation [13,14]. Mitochondrial respiration

Correspondence: Professor Salvatore Cuzzocrea, Department of Clinical and Experimental Medicine and Pharmacology, School of Medicine, University of Messina, Torre Biologica, Policlinico Universitario Via C. Valeria, Gazzi, 98100 Messina, Italy. Tel: (39) 090 2213644. Fax: (39) 090 2213300. Email: salvator@unime.it

ISSN 1071-5762 print/ISSN 1029-2470 online
DOI: 10.1080/10715760902954126

is directly inhibited by $ONOO^-$ and is an early marker of its cytotoxic effects [12]. Moreover, $ONOO^-$ can also cause DNA damage resulting in the activation of the nuclear enzyme poly-(ADP-ribose) polymerase (PARP). The excessive activation of PARP in turn results in depletion of NAD and ATP and ultimately neuronal death [9].

Several antioxidants showed neuroprotection in SCI and in associated conditions like oxidative stress and inflammation [3,9,15].

Peroxynitrite is known to undergo acid-catalysed decomposition by two distinct pathways [16,17]. Several studies have reported that certain water-soluble iron (III) porphyrins are highly active $ONOO^-$ decomposition catalysts, catalysing the isomerization of $ONOO^-$ almost exclusively to nitrate [18,19].

Moreover, it has been recognized that water-soluble iron (III) porphyrin derivatives are highly reactive toward peroxynitrite with rate constants as high as $5.0 \times 10^7\,M^{-1}\,s^{-1}$ [20]. These agents catalyse the isomerization of peroxynitrite, resulting in its decomposition to the less reactive anion, nitrate, thereby decreasing the levels of the potent oxidizing and nitrating species, peroxynitrite. In previous studies, iron (III) metalloporphyrin-based peroxynitrite decomposition catalysts, including 5,10,15,20-tetrakis-[4-sulphonatophenyl]-porphyrinato-iron[III] and FeCl tetrakis-2-(triethylene glycol monomethyl ether) pyridyl porphyrin have been shown to have protection in models of myocardial infarction [21] and cytokine-induced [22] or doxorubicin-induced [23] or endotoxin-induced [24] cardiac dysfunction. In addition, recently we have demonstrated that 5,10,15,20-tetrakis(4-sulphonatophenyl)porphyrinato iron III chloride (FeTSPP), a peroxynitrite decomposition catalyst, significantly reduced the development of SCI [25]. In the present study, we examined the anti-inflammatory and anti-apoptotic mechanisms of action of the novel metalloporphyrinic peroxynitrite decomposition catalyst ww-85 in a mouse model of secondary injury in the spinal cord. In particular, we have determined the following endpoints of the inflammatory response: (1) histological damage, (2) motor recovery, (3) neutrophil infiltration, (4) NF-κB expression, (5) nitrotyrosine formation and PARP activation, (6) apoptosis as TUNEL staining and (7) Bax and Bcl-2 expression.

Materials and methods

Animals

Male adult CD1 mice (25–30 g, Harlan Nossan, Milan, Italy) were housed in a controlled environment and provided with standard rodent chow and water. Animal care was in compliance with Italian regulations on protection of animals used for experimental and other scientific purpose (D.M. 116192) as well as with the EEC regulations (O.J. of E.C. L 358/1 12/18/1986).

SCI

Mice were anaesthetized using chloral hydrate (400 mg/kg body weight). A longitudinal incision was made on the midline of the back, exposing the paravertebral muscles. These muscles were dissected away exposing T5–T8 vertebrae. The spinal cord was exposed via a four-level T5–T8 laminectomy and SCI was produced by extradural compression of the spinal cord using an aneurysm clip with a closing force of 24 g. Following surgery, 1.0 cc of saline was administered subcutaneously in order to replace the blood volume lost during the surgery. During recovery from anaesthesia, mice were placed on a warm heating pad and covered with a warm towel. Mice were singly housed in a temperature-controlled room at 27°C for a survival period of 10 days. Food and water were provided to the mice *ad libitum*. During this time period, the animals' bladders were manually voided twice a day until the mice were able to regain normal bladder function. In all injured groups, the spinal cord was compressed for 1 min. Sham animals were only subjected to laminectomy.

Experimental design

A dose–response effect was performed investigating the effect of ww-85 (30–300 μg/kg, i.p.) on the development of SCI. Mice were randomized into 10 groups. Sham animals were subjected to the surgical procedure, except that the aneurysm clip was not applied and treated 1 h after surgical procedure intraperitoneally (i.p.) with vehicle (saline) or ww-85 (30–300 μg/kg, i.p.). The remaining mice were subjected to SCI (as described above) and treated with an i.p. bolus of vehicle (saline) or ww-85 (30–300 μg/kg, i.p.) 1 h after SCI. The doses of ww-85 (30–300 μg/kg, i.p.) used here were based on a previous *in vivo* study [26]. In the experiments regarding the motor score the animals were treated as previously described and daily until day 10.

Myeloperoxidase activity

Myeloperoxidase (MPO) activity, an indicator of polymorphonuclear leukocyte (PMN) accumulation, was determined in the spinal cord tissues as previously described [27] at 24 h after SCI. MPO activity was defined as the quantity of enzyme degrading 1 μmol of peroxide/min at 37°C and was expressed in milliunits/g of wet tissue.

Thiobarbituric acid-reactant substances measurement

Thiobarbituric acid-reactant substances measurement, which is considered a good indicator of lipid

peroxidation, was determined, as previously described [28] in the spinal cord tissue at 24 h after SCI. Thiobarbituric acid-reactant substances were calculated by comparison with OD_{650} of standard solutions of 1,1,3,3-tetramethoxypropan 99% malondialdehyde bis (dymethyl acetal) 99% (MDA) (Sigma, Milan). The absorbance of the supernatant was measured by spectrophotometry at 650 nm.

Lipid peroxidation

Lipid peroxides (LPO) were measured in portions of spinal cord tissues, collected at 24 h after SCI, by using LPO determination kit (OXIS International Inc., USA) according to the manufacturer instructions.

Light microscopy

Spinal cord biopsies were taken at 24 h following trauma. Tissue segments containing the lesion (1 cm on each side of the lesion) were paraffin embedded and cut into 5-μm-thick sections. Tissue longitudinal sections (thickness 5 μm) were deparaffinized with xylene, stained with Haematoxylin/Eosin (H&E), with Gomori stain and studied using light microscopy (Dialux 22 Leitz).

The segments of each spinal cord were evaluated in the rostral/caudal perilesional area by an experienced histopathologist (RO). Damaged neurons were counted and the histopathology changes of the gray matter were scored on a 6-point scale [29]: 0, no lesion observed, 1, gray matter contained 1–5 eosinophilic neurons; 2, gray matter contained 5–10 eosinophilic neurons; 3, gray matter contained more than 10 eosinophilic neurons; 4, small infarction (less than one third of the gray matter area); 5, moderate infarction (one third to one half of the gray matter area); 6, large infarction (more than half of the gray matter area). The scores from all the sections from each spinal cord were averaged to give a final score for individual mice. All the histological studies were performed in a blinded fashion.

Immunohistochemical localization of nitrotyrosine, PAR, FAS-ligand, Bax and Bcl-2

Spinal cord biopsies were taken at 24 h following trauma. Tissue segments containing the lesion (1 cm on each side of the lesion, rostrally/caudally to the perilesional area) were paraffin embedded and cut into 5-μm-thick sections. Tissue longitudinal sections (thickness 5 μm), after deparaffinization, endogenous peroxidase was quenched with 0.3% (v/v) hydrogen peroxide in 60% (v/v) methanol for 30 min. The sections were permeabilized with 0.1% (w/v) Triton X-100 in PBS for 20 min. Non-specific adsorption was minimized by incubating the section in 2% (v/v) normal goat serum in PBS for 20 min. Endogenous biotin or avidin binding sites were blocked by sequential incubation for 15 min with biotin and avidin (DBA), respectively. Sections were incubated overnight with anti-Fas-ligand (1:500 in PBS, v/v), anti-nitrotyrosine rabbit polyclonal antibody (Upstate, 1:500 in PBS, v/v), anti-PAR antibody (Bio-Mol, 1:200 in PBS, v/v), anti-Bax antibody (Santa Cruz Biotechnology, 1:500 in PBS, v/v) or with anti-Bcl-2 polyclonal antibody (Santa Cruz Biotechnology, 1:500 in PBS, v/v). Sections were washed with PBS and incubated with secondary antibody. Specific labelling was detected with a biotin-conjugated goat anti-rabbit IgG and avidin-biotin peroxidase complex (DBA). To verify the binding specificity for nitrotyrosine, PAR, Fas-ligand, Bax and Bcl-2, some sections were also incubated with only the primary antibody (no secondary) or with only the secondary antibody (no primary). In these situations no positive staining was found in the sections indicating that the immunoreactions were positive in all the experiments carried out.

Immunocytochemistry photographs ($n = 5$) were assessed by densitometry by using Imaging Densitometer (AxioVision, Zeiss, Milan, Italy) and a computer program. In particular the densitometry analysis was carried out in longitudinal section in which the spinal cord was orientated in order to observe the lesion area as well as the rostrally/caudally perilesional area. In this type of section, is possible to evaluate the presence/absence or the alteration of the distribution pattern. Therefore, the densitometry data obtained represent all these difference.

Terminal deoxynucleotidyltransferase-mediated UTP end labelling (TUNEL) assay

TUNEL assay was conducted by using a TUNEL detection kit according to the manufacturer's instruction (Apotag, HRP kit DBA, Milan, Italy). Briefly, tissue segments containing the lesion (1 cm on each side of the lesion, rostrally/caudally to the perilesional area) were cut into longitudinal 5-μm-thick sections. Tissue were incubated with 15 μg/ml proteinase K for 15 min at room temperature and then washed with PBS. Endogenous peroxidase was inactivated by 3% H_2O_2 for 5 min at room temperature and then washed with PBS. Sections were immersed in terminal deoxynucleotidyltransferase (TdT) buffer containing deoxynucleotidyl transferase and biotinylated dUTP in TdT buffer, incubated in a humid atmosphere at 37°C for 90 min and then washed with PBS. The sections were incubated at room temperature for 30 min with anti-horseradish peroxidase-conjugated antibody and the signals were visualized with diaminobenzidine. The number of TUNEL positive cells/high-power field was counted in 5–10 fields for each coded slide.

Measurement of TNF-α and IL-1β̃

Portions of spinal cord tissues, containing the lesion (1 cm on each side of the lesion, rostrally/caudally to the perilesional area), collected at 24 h after SCI, were homogenized as previously described in PBS containing 2 mmol/L of phenyl-methyl sulphonyl fluoride (Sigma Chemical Co.) and tissue TNFα and IL-1β levels were evaluated. The assay was carried out by using a colorimetric, commercial kit (Calbiochem-Novabiochem Corporation, USA) according to the manufacturer instructions. All TNFα and IL-1β determinations were performed in duplicate serial dilutions.

Preparation of spinal cord extracts and Western blot analysis for IκB-α, phospho-NF-κB p65 (serine 536), NF-κB p65, Bax and Bcl-2

Cytosolic and nuclear extracts were prepared as previously described [30] with slight modifications. Briefly, spinal cord tissues from each mouse containing the lesion (1 cm on each side of the lesion, rostrally/caudally to the perilesional area) were suspended in extraction Buffer A containing 0.2 mM PMSF, 0,15 μM pepstatin A, 20 μM leupeptin, 1 mM sodium orthovanadate, homogenized at the highest setting for 2 min and centrifuged at 1000 x g for 10 min at 4°C. Supernatants represented the cytosolic fraction. The pellets, containing enriched nuclei, were re-suspended in Buffer B containing 1% Triton X-100, 150 mM NaCl, 10 mM TRIS-HCl pH 7.4, 1 mM EGTA, 1 mM EDTA, 0.2 mM PMSF, 20 μM, 0.2 mM sodium orthovanadate. After centrifugation for 30 min at 15 000 x g at 4°C, the supernatants containing the nuclear protein were stored at −80°C for further analysis. The levels of IκB-α, phospho-NF-κB p65 (serine 536), Bax and Bcl-2 were quantified in cytosolic fraction from spinal cord tissue collected 24 h after SCI, while NF-κB p65 levels were quantified in nuclear fraction. The filters were blocked with 1 × PBS, 5% (w/v) non-fat dried milk for 40 min at room temperature and subsequently probed with specific Abs IκB-α (Santa Cruz Biotechnology, 1:1000) or phospho-NF-κB p65 (serine 536) (Cell Signaling, 1:1000) or anti-Bax (1:500; Santa Cruz Biotechnology) or anti-Bcl-2 (1:500; Santa Cruz Biotechnology) or anti- NF-κB p65 (1:1000; Santa Cruz Biotechnology) in 1 × PBS, 5% w/v non-fat dried milk, 0.1% Tween-20 (PMT) at 4°C, overnight. Membranes were incubated with peroxidase-conjugated bovine anti-mouse IgG secondary antibody or peroxidase-conjugated goat anti-rabbit IgG (1:2000, Jackson ImmunoResearch, West Grove, PA) for 1 h at room temperature.

To ascertain that blots were loaded with equal amounts of proteic lysates, they were also incubated in the presence of the antibody against β-actin protein (1:10 000 Sigma-Aldrich Corp.). The relative expression of the protein bands of IκB-α (∼37 kDa), phospho NF-κB (∼65 kDa), NF-κB p65 (∼75 kDa), Bax (∼23 kDa), Bcl-2 (∼29 kDa) was quantified by densitometric scanning of the X-ray films with a GS-700 Imaging Densitometer (GS-700, Bio-Rad Laboratories, Milan, Italy) and a computer program (Molecular Analyst, IBM) were quantified by scanning densitometry (Imaging Densitometer GS-700 BIO-RAD, USA).

Grading of motor disturbance

The motor function of mice subjected to compression trauma was assessed once a day for 10 days after injury. Recovery from motor disturbance was graded using the modified murine Basso, Beattie and Bresnahan (BBB) [31] hind limb locomotor rating scale [32,33].

Materials

The ww-85 was obtained from Inotek Pharmaceuticals Corporation (Beverly, USA). All other compounds were obtained from Sigma-Aldrich Company Ltd. (Milan, Italy). All other chemicals were of the highest commercial grade available. All stock solutions were prepared in non-pyrogenic saline (0.9% NaCl; Baxter, Italy, UK).

Statistical evaluation

All values in the figures and text are expressed as mean ± standard error of the mean (SEM) of n observations. For the *in vivo* studies, n represents the number of animals studied. In the experiments involving histology or immunohistochemistry, the figures shown are representative of at least three experiments performed on different experimental days. The results were analysed by one-way ANOVA followed by a Bonferroni *post-hoc* test for multiple comparisons. A p-value of less than 0.05 was considered significant. BBB scale data were analysed by the Mann-Whitney test and considered significant when p-value was < 0.05.

Results

ww-85 reduces the severity of spinal cord trauma

The severity of the trauma at the level of the perilesional area assessed the presence of oedema as well as alteration of the white matter (Figure 1A and D) and was evaluated at 24 h after injury. Significant damage to the spinal cord was observed in the spinal cord tissue from SCI mice when compared with sham-operated mice (Figure 1A). Notably, a significant protection against the spinal cord injury was observed in ww-85 (300 μg/kg) treated mice (Figure 1C and D). In sham animals (Figure 1E), a significant presence of Gomori-positive were observed in the astrocytes as well as in the vessels. At 24 h after the injury, a significant loss of the Gomori positive localization was observed in the spinal cord tissues in

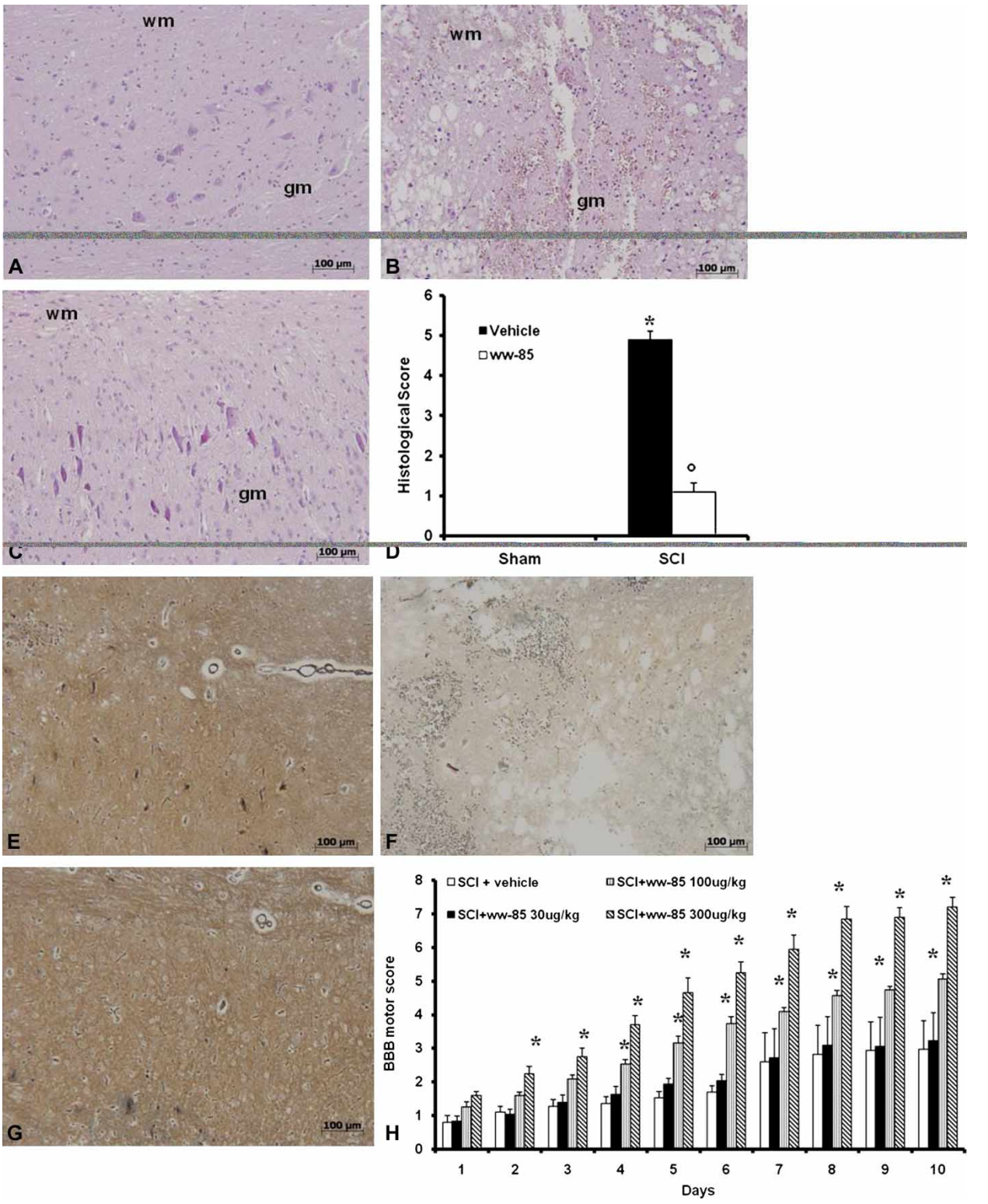

Figure 1. Effect of ww-85 on histological alterations of the spinal cord tissue 24 h after injury. No histological alterations (A) were observed in the spinal cord tissues from sham-operated mice. Twenty-four hours after trauma a significant damage to the spinal cord, from no-treated SCI operated ?mice at the perilesional area, was assessed by the presence of oedema as well as alteration of the white matter (B). Notably, a significant protection from the SCI was observed in the tissue collected from ww-85 SCI treated mice (C). The histological score (D) was made by an independent observer. A significant presence of Gomori-positive localization was observed in the astrocytes and in the vessels of sham-operated mice (E). At 24 h after the injury in no-treated SCI operated ? mice (F), a significant loss of presence of Gomori-positive localization was observed. In contrast, in the tissue collected from ww-85 SCI treated mice there was an evident presence of Gomori-positive localization (G). In addition, the degree of motor disturbance was assessed every day until 10 days after SCI by Basso, Beattie and Bresnahan criteria (H). The treatment with ww-85 ameliorated the recovery of motor disturbance after SCI in a dose dependent fashion (h). wm: White matter; gm: gray matter. This figure is representative of at least three experiments performed on different experimental days. Values shown are mean ± SE mean of 10 mice for each group. $*p < 0.01$ vs SCI.

mice subjected to SCI? (Figure 1F). In contrast, in ww-85 (300 μg/kg) treated mice the loss of Gomori positive localization was attenuated in the central part of lateral and dorsal funiculi (Figure 1G). In order to evaluate if histological damage to the spinal cord was associated with a loss of motor function, the modified BBB hind limb locomotor rating scale score was evaluated. While motor function was only slightly impaired in sham mice, mice subjected to SCI had significant deficits in hind limb movement. ww-85 (30, 100, 300 μg/kg) reduced the degree of limb motor disturbances induced by SCI (Figure 1H).

Effects of ww-85 on neutrophil infiltration

The above-mentioned histological pattern of spinal cord injury appeared to be correlated with the influx of leukocytes into the spinal cord. Therefore, we investigated the effect of ww-85 on the neutrophil infiltration by measuring tissue myeloperoxidase (MPO) activity (Figure 2). MPO activity was significantly elevated in the spinal cord at 24 h after injury in mice subjected to SCI when compared with sham-operated mice (Figure 2). Treatment with ww-85 attenuated neutrophil infiltration into the spinal cord at 24 h after injury in a dose-dependent fashion (Figure 2).

Effects of ww-85 on nitrotyrosine formation, lipid peroxidation and PAR formation after SCI

Twenty-four hours after SCI, nitrotyrosine, a specific marker of nitrosative stress, was measured by immunohistochemical analysis in the spinal cord sections to determine the localization of 'peroxynitrite formation' and/or other nitrogen derivatives produced during SCI. Spinal cord sections from sham-operated mice did not stain for nitrotyrosine (data not shown), whereas spinal cord sections obtained from SCI mice exhibited positive staining for nitrotyrosine (Figure 3A and C). The positive staining was mainly localized in inflammatory cells as well as in nuclei of Schwann cells in the white and gray matter of the spinal cord tissues. ww-85 treatment (300 μg/kg) reduced the degree of positive staining for nitrotyrosine (Figure 3B and C) in the spinal cord. In addition, at 24 h after SCI, thiobarbituric acid-reactant substances levels and lipid peroxides (LPO) were also measured in the spinal cord tissue as an indicator of lipid peroxidation. A significant increase of thiobarbituric acid-reactant substances (Figure 3D) and LPO levels (Figure 3E) were observed in the spinal cord collected at 24 h from mice subjected to SCI when compared with sham-operated mice. Thiobarbituric acid-reactant substances (Figure 3D) and LPO levels (Figure 3E) were significantly attenuated in a dose-dependent fashion by the intraperitoneal injection of ww-85. Infiltration of leukocytes into the white matter has been suggested to contribute significantly to the SCI releasing free oxygen and nitrogen radicals and favouring PARP activation [34]. In our study, immunohistochemistry for PAR, as an indicator of *in vivo* PARP activation, revealed the occurrence of positive staining for PAR localized in nuclei of Schwann cells in the white and gray matter of the spinal cord tissues from mice subjected to SCI (Figure 3F and H). ww-85 treatment (300 μg/kg) reduced the degree of positive staining for PAR (Figures G and H) in the spinal cord.

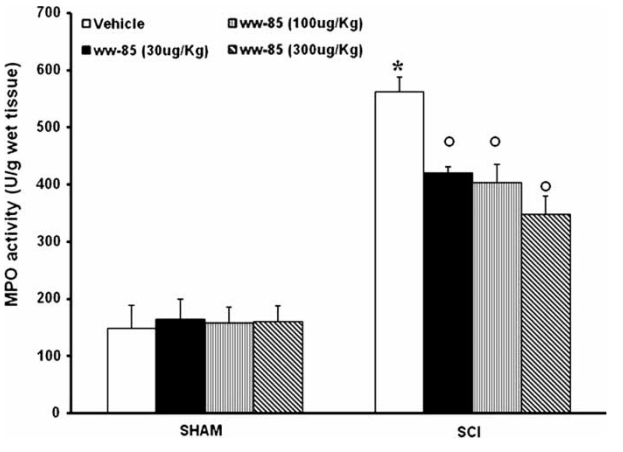

Figure 2. Effects of ww-85 on MPO activity. Following the injury, MPO activity in spinal cord from SCI mice was significantly increased at 24 h after the damage in comparison to sham mice. Treatment with ww-85 attenuated neutrophil infiltration into the spinal cord in a dose-dependent fashion. Data are means ± SE means of 10 mice for each group. $^{\star}p < 0.01$ vs Sham. $^{\circ}p < 0.01$ vs SCI + vehicle.

Effect of ww-85 on IκB-α degradation, phosphorylation of Ser536 on p65, expression of NF-κB p65 and NF-κB translocation

We evaluated IκB-α degradation, phosphorylation of Ser536 on the NF-κB sub-unit p65, total NF-κB p65 by Western Blot analysis to investigate the cellular mechanisms by which treatment with ww-85 may attenuate the development of SCI.

A basal level of IκB-α was detected in the spinal cord from sham-operated animals, whereas in SCI mice IκB-α levels were substantially reduced. ww-85 treatment (300 μg/kg) prevented the SCI-induced IκB-α degradation (Figure 4A and A_1). In addition, SCI caused a significant increase in the phosphorylation of Ser536 at 24 h (Figure 4B and B_1). The treatment with ww-85 (300 μg/kg) significantly reduced the phosphorylation of p65 on Ser536 (Figure 4B and B_1). Moreover, NF-κB p65 levels in the nuclear fractions of the spinal cord tissue were also significantly increased at 24 h after SCI compared to the sham-operated mice (Figure 4C and C_1). ww-85 (300 μg/kg) treatment significantly reduced the levels of NF-κB p65 protein as shown in Figure 4C and C_1.

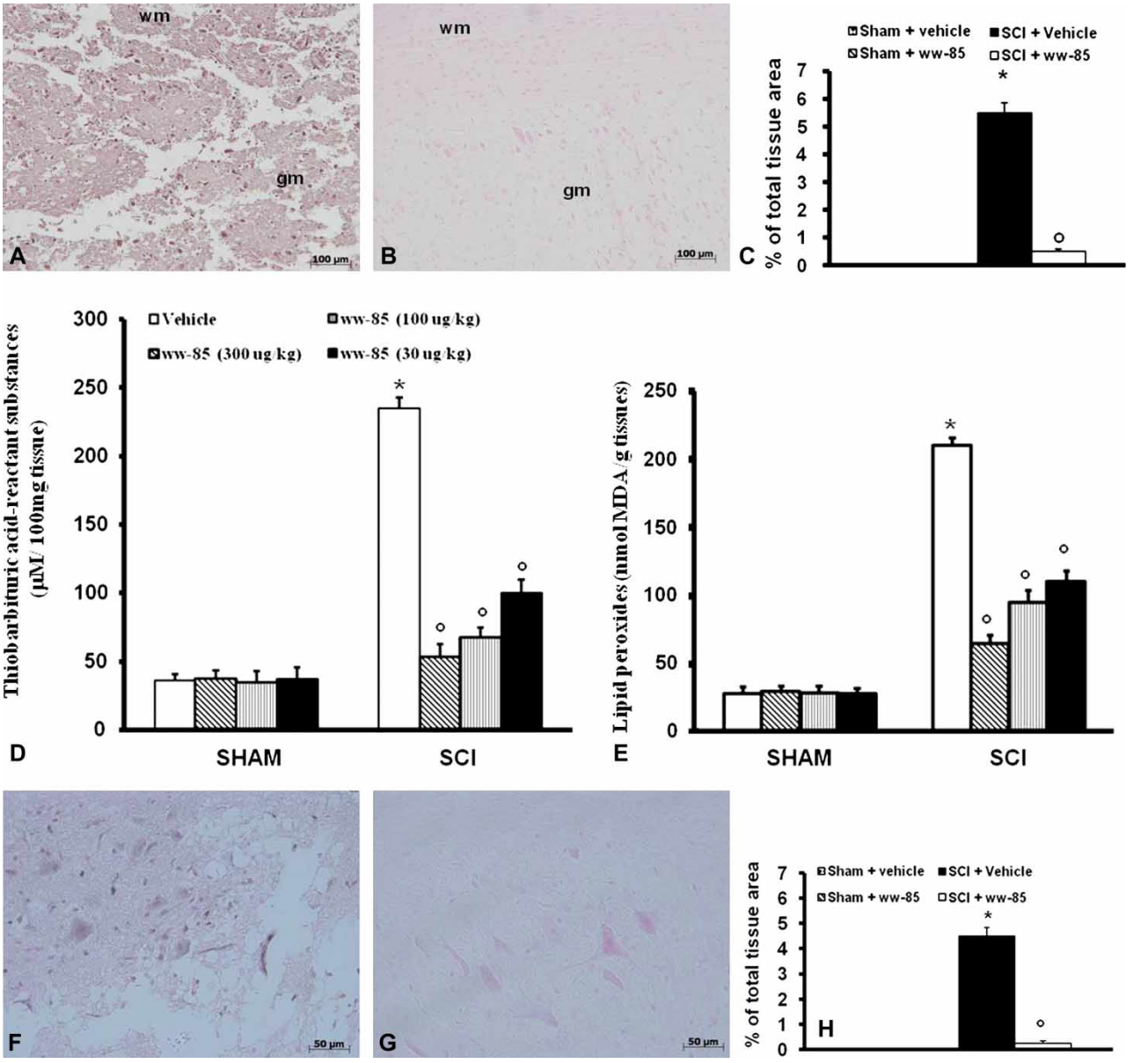

Figure 3. Effects of ww-85 on nitrotyrosine formation, lipid peroxidation and PARP activation. In tissue sections obtained from vehicle-treated animals after SCI demonstrate positive staining for nitrotyrosine mainly localized in inflammatory, in nuclei of Schwann cells in the white and gray matter (A). ww-85 treatment (300 µg/kg) reduced the degree of positive staining for nitrotyrosine (B) in the spinal cord. Densitometry analysis of immunocytochemistry photographs ($n=5$ photos from each sample collected from all mice in each experimental group) for nitrotyrosine (C) from spinal cord tissues was assessed. Data are expressed as percentage of total tissue area. In addition, a significant increase of thiobarbituric acid-reactant substances (D) and lipid peroxides (LPO) (E) were observed in the spinal cord collected at 24 h from mice subjected to SCI when compared with sham-operated mice. Thiobarbituric acid-reactant substances (D) and LPO levels (E) were significantly attenuated in a dose-dependent fashion by the intraperitoneal injection of ww-85. In addition, immunohistochemistry for PAR, an indicator of *in vivo* PARP activation, revealed the occurrence of positive staining for PAR localized in nuclei of Schwann cells in wm and gm of the spinal cord tissues from SCI mice (F). ww-85 treatment (300 µg/kg) reduced the degree of positive staining for PAR (G) in the spinal cord. Densitometry analysis of immunocytochemistry photographs ($n=5$ photos from each sample collected from all mice in each experimental group) for PAR (H) from spinal cord tissues was assessed. Data are expressed as percetage of total tissue area. These figures are representative of at least three experiments performed on different experimental days. Data are means ± SE means of 10 mice for each group. $^{*}p<0.01$ vs Sham. $^{\circ}p<0.01$ vs SCI + vehicle.

Effect of ww-85 modulate the expression of tnf-α and IL-1β after SCI

To test whether ww-85 may modulate the inflammatory process through the regulation of the secretion of pro-inflammatory cytokines, we analysed the spinal cord tissue levels of TNF-α and IL-1β. A substantial increase in TNF-α and IL-1β production was found in spinal cord tissues samples collected from SCI mice at 24 h after SCI (Figure 5A and D, respectively). Spinal cord levels of TNF-α and IL-1β were significantly attenuated in a dose-dependent fashion by the intraperitoneal injection of ww-85 (Figure 5B and E, respectively).

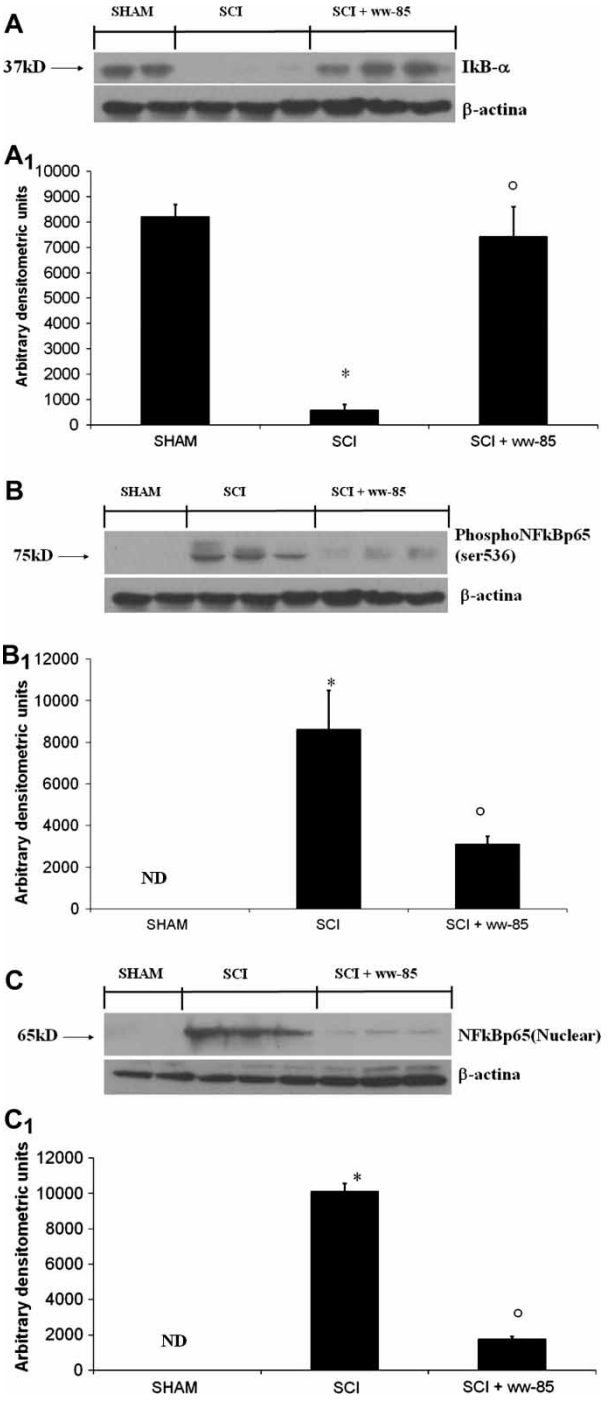

Figure 4. Effects of ww-85 treatment on IκB-α degradation, phosphorylation of Ser536 on the NF-κB sub-unit p65, total NF-κB p65. By Western Blot analysis, a basal level of IκB-α was detected in the spinal cord from sham-operated animals, whereas in SCI mice IκB-α levels were substantially reduced. ww-85 treatment (300 μg/kg) prevented the SCI-induced IκB-α degradation (A, A_1). In addition, SCI caused a significant increase in the phosphorylation of Ser536 at 24 h (B, B_1) and in nuclear NF-kB p65 compared to the sham-operated mice (C, C_1). ww-85 treatment (300 μg/kg) significantly reduced the phosphorylation of p65 on Ser536 (B, B_1) and NF-kB p65 levels as shown in (C) and (C_1). Immunoblotting in (A–C) is representative of one spinal cord tissues out of 5–6 analysed. The results in (A_1, B_1 and C_1) are expressed as mean ± SEM from 5–6 spinal cord tissues. $^{\star}p < 0.01$ vs Sham; $^{\circ}p < 0.01$ vs SCI.

Effects of ww-85 on modulates expression of FAS ligand after SCI

Immunohistological staining for FAS ligand in the spinal cord was also determined 24 h after injury. Sections of spinal cord from sham-operated mice did not stain for FAS ligand (data not shown), whereas spinal cord sections obtained from SCI-treated mice exhibited positive staining for FAS ligand (Figure 6A, see densitometric analysis c). The positive staining was localized in various cells in the gray matter. ww-85 treatment (300 μg/kg) reduced the degree of positive staining for FAS-ligand (Figure 6B and C) in the spinal cord.

Effects of ww-85 on apoptosis in spinal cord after injury

To test whether spinal cord damage was associated to cell death by apoptosis, we measured TUNEL-like staining in the perilesional spinal cord tissue. Almost no apoptotic cells were detected in the spinal cord from sham-operated mice (Figure 7A, see apoptotic cell count d). At 24 h after the trauma, tissues from SCI control mice demonstrated a marked appearance of dark brown apoptotic cells and intercellular apoptotic fragments (Figure 7B, see apoptotic cell count d). In contrast, tissues obtained from mice treated with ww-85 (300 μg/kg) (Figure 7C, see apoptotic cell count c) demonstrated no apoptotic cells or fragments.

Western blot analysis and immunohistochemistry for Bax and Bcl-2

At 24 h after SCI, the appearance of Bax in spinal cord homogenates was investigated by Western blot. Bax levels were appreciably increased in the spinal cord from mice subjected to SCI (Figure 8A and A_1). On the contrary, ww-85 treatment (300 μg/kg) prevented the SCI-induced Bax expression (Figure 8A and A_1).

By Western blot analysis was also analysed Bcl-2 expression in homogenates from spinal cord of each mice. A basal level of Bcl-2 expression was detected in spinal cord from sham-operated mice (Figure 8B and B_1). Twenty-four hours after SCI, the Bcl-2 expression was significantly reduced in spinal cord from SCI mice (Figure 8B and B_1). Treatment of mice with ww-85 (300 μg/kg) significantly reduced the SCI-induced inhibition of Bcl-2 expression (Figure 8B and B_1).

Moreover, samples of spinal cord tissue were taken at 24 h after SCI in order to determine the immunohistological staining for Bax and Bcl-2. Sections of spinal cord from sham-operated mice did not stain for Bax (data not shown), whereas spinal cord sections obtained from SCI mice exhibited a positive staining for Bax (Figure 8C and E). ww-85 (300 μg/kg)

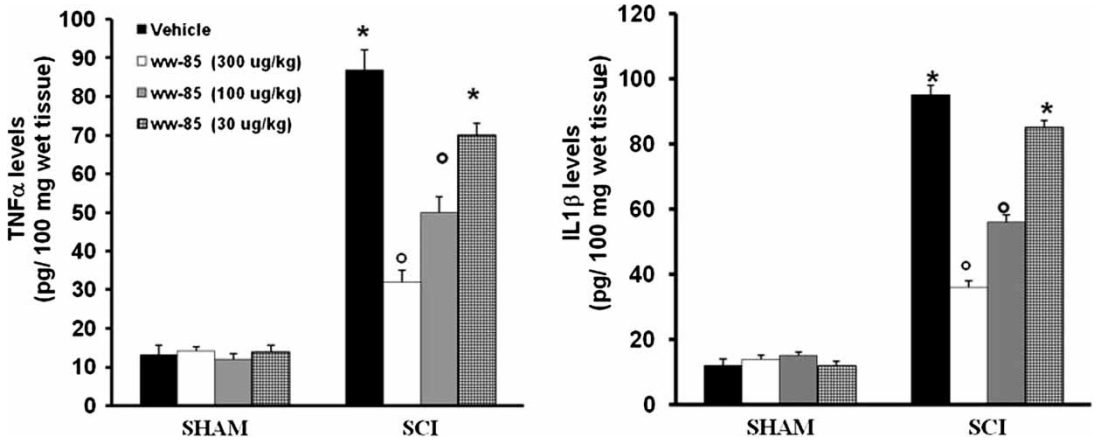

Figure 5. Effects of ww-85 treatment on immunohistochemical localization of TNF-α and IL-2. Spinal cord sections were processed at 24 h after SCI to determine the immunohistological staining for tnf-α and IL-1β expression. A substantial increase in TNF-α (A) and IL-1β (D) expression was found in inflammatory cells, in nuclei of Schwann cells in wm and gm of the spinal cord tissues from SCI mice at 24 h after SCI. Spinal cord levels of TNF-α (B) and IL-1β (E) were significantly attenuated in ww-85 (300 μg/kg)-SCI treated mice in comparison to SCI animals. Densitometry analysis of immunocytochemistry photographs ($n=5$ photos from each sample collected from all mice in each experimental group) for IL-2 (C) and for TNF-α (F) from spinal cord tissues was assessed. Data are expressed as percentage of total tissue area. This figure is representative of at least three experiments performed on different experimental days. $^{\star}p<0.01$ vs Sham. $^{\circ}p<0.01$ vs SCI+vehicle.

treatment reduced the degree of positive staining for Bax in the spinal cord of mice subjected to SCI (Figure 8D and E). In addition, spinal cord sections from sham-operated mice demonstrated Bcl-2 positive staining (data not shown) while in SCI control mice the staining significantly reduced (Figure 8F and H). ww-85 (300 μg/kg) treatment attenuated the loss of positive staining for Bcl-2 in the spinal cord from SCI- subjected mice (Figure 8G and H).

Discussion

Primary injury to the adult spinal cord is irreversible, whereas secondary degeneration is delayed and therefore amenable to intervention. Accordingly, several studies have shown that therapies targeting various factors involved in the secondary degeneration cascade lead to tissue sparing and improved behavioural outcomes in spinal cord-injured animals [3,34–36].

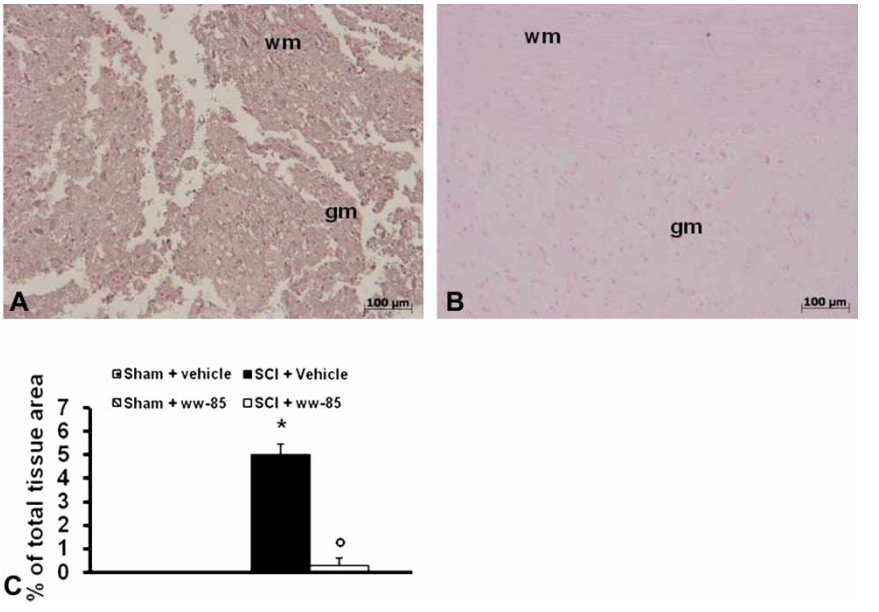

Figure 6. Effects of ww-85 treatment on immunohistochemical localization and expression of Fas-ligand. Spinal cord sections were processed at 24 h after SCI to determine the immunohistological staining for Fas-ligand. No positive staining for FAS ligand was present in tissue sections obtained from sham groups (data not shown). A substantial increase in Fas-ligand expression was found in inflammatory cells (A) in wm and gm of the spinal cord tissues from SCI-operated mice. Spinal cord levels of Fas-ligand (B) were significantly reduced in ww-85 (300 μg/kg)-SCI treated mice in comparison to SCI-operated mice. Densitometry analysis of immunocytochemistry photographs ($n=5$ photos from each sample collected from all mice in each experimental group) for Fas-ligand (C) from spinal cord tissues was assessed. Data are expressed as percentage of total tissue area. This figure is representative of at least three experiments performed on different experimental days. $^{\star}p<0.01$ vs Sham. $^{\circ}p<0.01$ vs SCI-IL WT mice; wm: white matter; gm: gray matter.

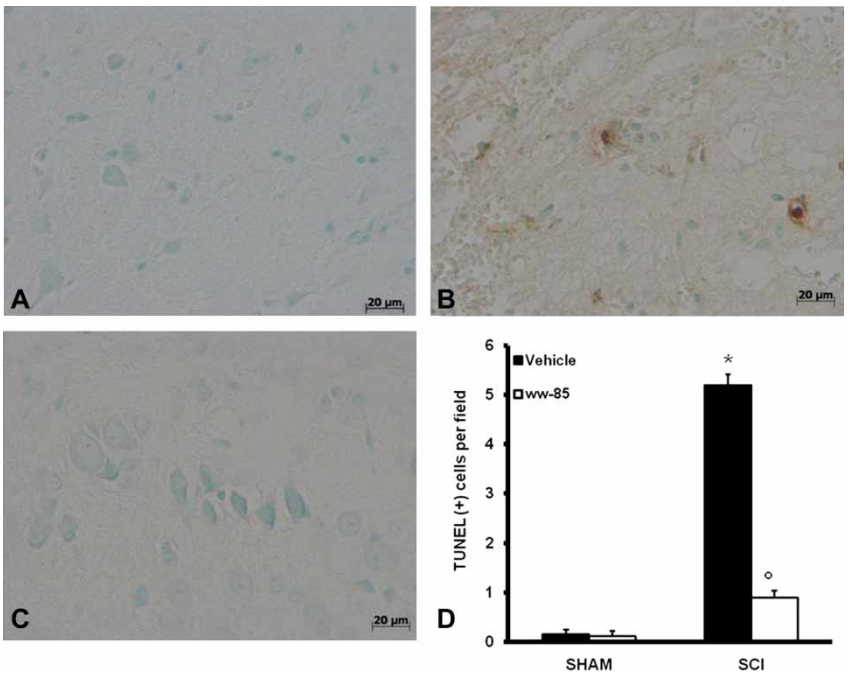

Figure 7. Effects of ww-85 treatment on TUNEL-like staining in the perilesional spinal cord tissue. Almost no apoptotic cells were detected in the spinal cord from sham mice (A). At 24 h after the trauma, SCI mice demonstrated a marked appearance of dark brown apoptotic cells and intercellular apoptotic fragments (B). In contrast, tissues obtained from mice treated with ww-85 (300 μg/kg) demonstrated no apoptotic cells or fragments (C). The number of TUNEL positive cells/high-power field was counted in 5–10 fields for each coded slide (D). This figure is representative of at least three experiments performed on different experimental days. $^{\star}p < 0.01$ vs Sham. $^{\circ}p < 0.01$ vs SCI-IL WT mice; wm: white matter; gm: gray matter.

Much of the damage that occurs in the spinal cord following traumatic injury is due to the secondary effects of glutamate excitotoxicity, Ca^{2+} overload and oxidative stress, three mechanisms that take part in a spiralling interactive cascade ending in neuronal dysfunction and death [10,37,38]. The role of reactive oxygen-induced oxidative damage to spinal cord lipids (i.e. lipid peroxidation) and proteins has been strongly supported in various studies [3,6,15,35]. Among the reactive oxygen species (ROS), $ONOO^-$ is known to play an important role in local and systemic inflammatory response as well as neurodegenerative disease [3,8,11,19].

The chemistry and biology of peroxynitrite have been significantly studied since its cytotoxic activity was first recognized [17,39–42]. This molecule has been implicated in local and systemic inflammatory response as well as neurodegenerative disease [3,8,11,19] and it has been shown that the body's own systems are ill-equipped to eliminate it [43].

A greater understanding of the role played by $ONOO^-$ in the pathogenesis of human disease will aid in the design of rational therapies for pharmacological intervention.

Metalloporphyrins are of particular interest for this reason; peroxynitrite reacts very efficiently with biological metal centres [44,45]. If a metalloporphyrin could be introduced into a living system as treatment for peroxynitrite injury, it would be of therapeutic potential. It has recently been shown that certain water-soluble manganese and iron porphyrins show high rates of reaction with peroxynitrite [42]. One such porphyrin, iron(III) meso-tetrakis(2,4,6-trimethyl-3,5-disulphonato) porphine chloride (FeTMPS) has already shown activity at micromolar levels and was shown to attenuate local inflammation [16] as well as SCI [25]. This result, combined with the attractive peroxynitrite turnover rates obtained for the family of pyridyl porphyrins, prompted us to consider a new catalyst based on the pyridyl porphyrin systems. The novel catalyst FP15, also called as 5,10,15,20-tetrakis[N-(benzyl-4′-carboxylate)pyridinium-2-yl]porphyrin iron(III) pentachloride, represents an effort to apply results obtained *in vitro* to biological systems [46]. This catalyst has been designed specifically for pharmacologic use, building on previous knowledge in the field for maximum efficacy [46]. The polyethylene glycol chains attached to the porphyrin provide a hydrophilic environment for peroxynitrite while providing sufficient bulk to hinder deleterious associations between the porphyrin and DNA [46]. It retains the high rate constant for peroxynitrite turnover observed for other iron porphyrin catalysts [47,48], showing that diverse groups may be introduced at the N-pyridyl position and the porphyrin will still retain activity [46]. The shape of the rate constant dependence on the catalyst concentration is non-linear and upward sloping and has been observed before for other FeTMPyP-based porphyrins [46,48].

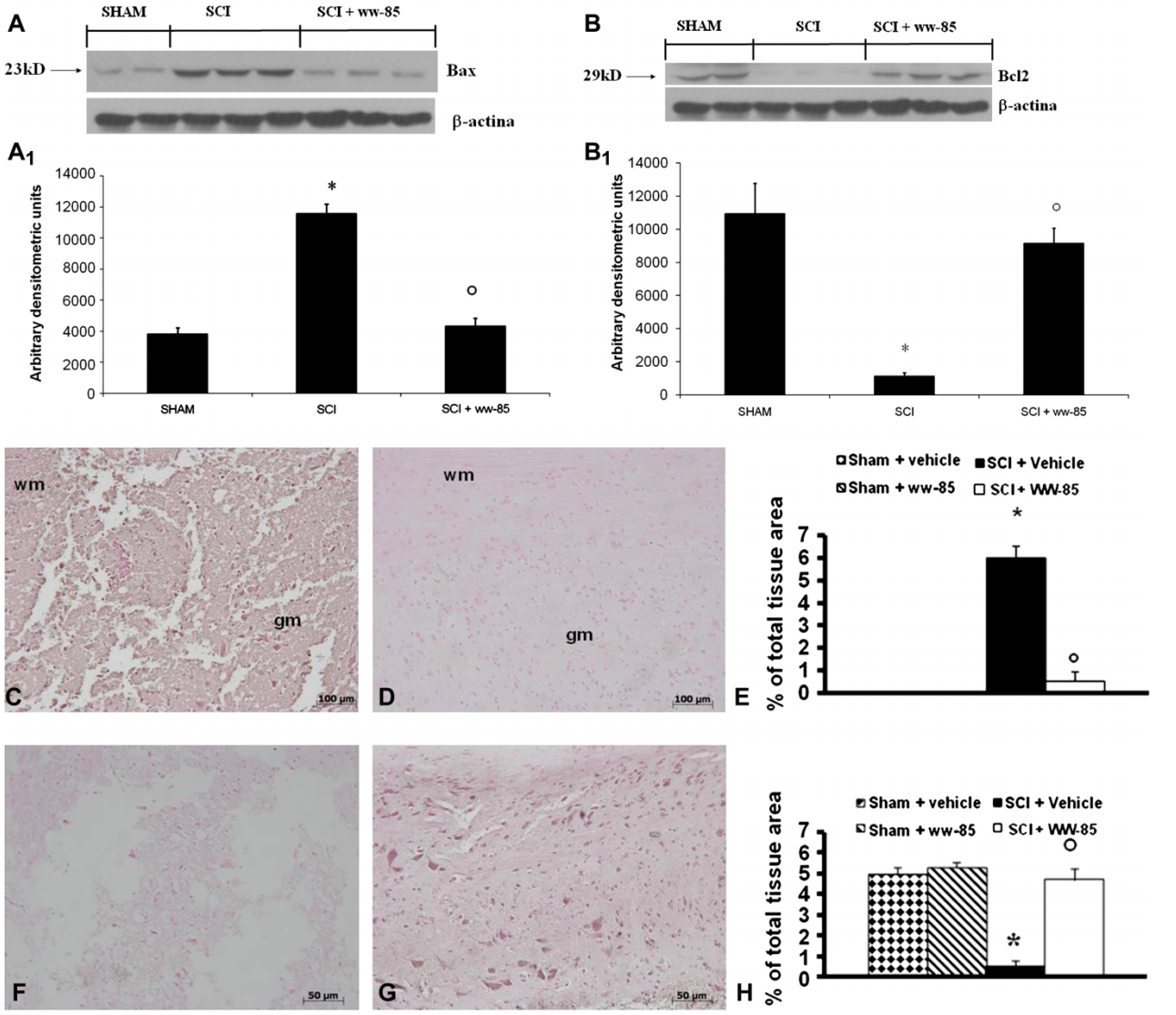

Figure 8. Effects of ww-85 treatment on expression of Bax and Bcl-2. By Western blot analysis, Bax levels were appreciably increased in the spinal cord from SCI mice (A and A_1). On the contrary, ww-85 (300 μg/kg) prevented the SCI-induced Bax expression (A and A_1). Moreover, a basal level of Bcl-2 expression was detected in spinal cord from sham-operated mice (B and B_1). Twenty-four hours after SCI, Bcl-2 expression was significantly reduced in spinal cord from SCI mice (B and B_1). ww-85 treatment (300 μg/kg) significantly reduced the SCI-induced inhibition of Bcl-2 expression (B and B_1). The results in (A_1) and (B_1) are expressed as mean ± SEM from $n = 5/6$ spinal cord for each group. *$p < 0.01$ vs sham, °$p < 0.01$ vs SCI + vehicle. By immunohistochemistry, SCI caused, at 24 h, an increase in the release of Bax expression (C). ww-85 (300 μg/kg) treatment reduced the degree of positive staining for Bax in the spinal cord (D). On the contrary, positive staining for Bcl-2 was observed in the spinal cord tissues from sham-operated mice (data not shown) while the staining was significantly reduced in SCI mice (F). ww-85 (300 μg/kg) attenuated the loss of positive staining for Bcl-2 in the spinal cord from SCI-subjected mice (G). Densitometry analysis of immunocytochemistry photographs ($n = 5$ photos from each sample collected from all mice in each experimental group) for Bax (E) and for Bcl-2 (H) from spinal cord tissues was assessed. Data are expressed as percentage of total tissue area. This figure is representative of at least three experiments performed on different experimental days. *$p < 0.01$ vs Sham. °$p < 0.01$ vs SCI + vehicle.

This investigation was designed to test whether the novel peroxynitrite decomposition catalyst WW-85 is useful to attenuate SCI, since it is known that ONOO− modulate the inflammatory response associated with SCI [25]. The present study showed that treatment with WW-85 significantly reduced spinal cord damage, (2) motor recovery, (3) neutrophil infiltration, (4) NF-κB expression, (5) nitrotyrosine formation and PARP activation, (6) apoptosis as TUNEL staining and (7) Bax and Bcl-2 expression. These findings confirm that ONOO− plays a crucial role in the pathology of SCI. Peroxynitrite is a potent nitrating species and initiator of lipid peroxidation and [49] apoptosis. Traditionally, immunodetection of nitrotyrosine has been used as evidence of peroxynitrite formation in biological tissue [50].

More recently, it has been shown that protein nitration may, under some conditions, arise independently of peroxynitrite via the action of MPO and nitrite [51].

In the present study we demonstrate that ww-85 attenuates the nitrotyrosine formation in the tissue

from SCI treated mice when compared with SCI+ vehicle mice. On the other hand, one cannot exclude the possible nitration of proteins via peroxynitrite-independent pathways. Indeed, myeloperoxidase in the presence of nitrite and H_2O_2 can cause nitration of proteins [52], whibh may be excluded in this study, since MPO was significantly reduced by WW-85. Based upon our current knowledge, it cannot be excluded that WW-85 may also contribute to peroxynitrite-independent pathways of protein nitration. Our results, however, are in line with previous findings using iron-based metalloporphyrinic agents as peroxynitrite decomposition catalysts which resulted in decreased myocardial myeloperoxidase activity in septic rats [24], decreased myeloperoxidase activity in lung reperfusion injury [53], decreased myeloperoxidase activity in model of IL-2 induced pulmonary toxicity [49] and decreased myeloperoxidase activity in the spinal cord tissues after SCI [25]. Nevertheless, our findings using the peroxynitrite decomposition catalyst WW-85 are significant in providing evidence that myeloperoxidase-derived nitration is probably not a major source of nitrotyrosine formation in this model of SCI.

One consequence of increased oxidative stress is the activation and inactivation of redox-sensitive proteins [54]. Recent evidence suggests that the activation of NF-κB may also be under the control of oxidant/antioxidant balance [55]. NF-κB is normally sequestered in the cytoplasm, bound to regulatory proteins IκBs. In response to a wide range of stimuli including oxidative stress, infection, hypoxia, extracellular signals and inflammation, IκB is phosphorylated by the enzyme IκB kinase [54]. The net result is the release of the NF-κB dimer, which is then free to translocate into the nucleus. The exact mechanisms by which ww-85 suppress NF-κB activation in inflammation are not known. We confirm here that SCI caused a significant increase in the phosphorylation of Ser536 on p65 in the spinal cord tissues at 24 h, whereas ww-85 treatment significantly reduced this phosphorylation. Moreover, we also demonstrate that the proxynitrite decomposition catalyst ww-85 inhibited the IκB-α degradation as well as the NF-κB translocation. Taken together, the balance between pro-inflammatory and pro-survival roles of NF-κB may depend on the phosphorylation status of p65 and $ONOO^-$ may play a central role in this process. NF-κB plays a central role in the regulation of many genes responsible for the generation of mediators or proteins in inflammation. These include the genes for TNF-α, IL-1β, iNOS and COX-2, to name but a few [56]. In this regard, it has been well demonstrated that in SCI the expression of proinflammatory cytokines (TNF-α and IL-1β) at the site of injury regulates the precise cellular events after SCI [57,58]. In the present study, we have clearly confirmed a significant increase in TNF-α and IL-1β in SCI. On the contrary, no significant expression of TNF-α and IL-1β was observed in the spinal cord sections obtained from SCI-operated mice which received ww-85 treatment confirming that $ONOO^-$ play an important role in the regulation of proinflammatory cytokines. This observation is in agreement with a previous study in which we have demonstrated ww-85 significantly reduced the expression of TNF-α and IL-1β in a model of rat cardiac transplant [26].

Large evidences indicate that TNF-α and IL-1β IL-2 also play an important role in the recruitment of inflammatory and immune cells in the injury site [1,59–62]. Moreover, immune and inflammatory cell infiltration to SCI sites is a major contributor to secondary degeneration [36,60,63–65]. In agreement with previous studies [60,65], we have observed in this experimental setting that the infiltration of neutrophils at the injury site 24 h following SCI is significantly increased in all animals. The neutrophils infiltration is reduced by the treatment with ww-85 confirming that $ONOO^-$ also play an important role in the regulation of neutrophils infiltration. Therefore, the inhibition of neutrophils infiltration by ww-85 described in the present study is likely to be due to the inhibition of proinflammatory cytokines expression.

Furthermore, various studies have demonstrated that, after SCI, apoptosis of neurons, oligodendrocytes and microglia occurs at the injury site as well as in distant areas of the spinal cord and brain [66–68]. Generation of free radicals and $ONOO^-$ by activated macrophages has also been implicated in causing oligodendrocyte apoptosis [69] and there is evidence that direct $ONOO^-$ formation is known to induce apoptosis in neuronal cells in culture [70]. We have demonstrated that the treatment with INOS-4885 attenuates the degree of apoptosis, measured by TUNEL detection kit in the spinal cord after the damage. Moreover, the observed attenuation of apoptosis by the ww-85 is also due to the prevention of lost of the anti-apoptotic pathway and reduction of pro-apoptotic pathway activation with a mechanism still to discover. Several studies [71] show that Bax gene plays an important role in cell death and CNS injury; moreover, other studies suggest that SCI-induced changes in Bcl-xL contribute considerably to neuronal death. We identified in the spinal cord injury pro-apoptotic transcriptional changes, including upregulation of pro-apoptotic Bax and down-regulation of anti-apoptotic Bcl-2, using western blot assay and by immunohystochemical staining. We report for the first time that ww-85 treatment reduced the signal for Bax in the treated group when compared with SCI+vehicle operated mice, while on the contrary, the signal is much more express for Bcl-2 in ww-85 treated mice than in SCI+vehicle operated mice.

Based on this evidence we clearly have shown that $ONOO^-$ interferes in the apoptotic process induced by SCI. However is not possible to exclude that anti-apoptotic effect observed after ww-85 treatment may be partially dependent on the attenuation of the inflammatory-induced damage. Further studies are needed in order to clarify these mechanisms.

However, recent data have demonstrated the induction of apoptosis in oligodendrocyte cells in response to $ONOO^-$ is PARP independent [72]. The role of PARP in apoptosis remains to be determined since conflicting data have been reported. It has been proposed that preventing PARP activation increased the sensitivity of cells to apoptosis-inducing agents [8]. Therefore, PARP undergoes site-specific proteolysis during apoptosis. In this regard, recently it has been demonstrated that PARP mediated-DNA repair is initiated in the cortex following experimental brain injury in rat acute post-traumatic period, but that subsequent PARP activation does not occur, possibly owing to delayed apoptosis-associated proteolysis, which may impair the repair of damaged DNA [73]. In addition, we have recently demonstrated that the two PARP inhibitors significantly prevent apoptosis in spinal cord injury [74]. In this study ww-85 significantly reduced the PAR formation, index of PARP activation, as well as the DNA damage in spinal cord tissue from mice subjected to trauma. Thus, our *in vivo* findings support the view that ww-85 by reduction of PARP activation induced by $ONOO^-$ prevent the activation of the apoptosis pathway.

Thus, we can hypothesize that the mechanism of this $ONOO^-$ decomposition catalyst may be related to a prevention of $ONOO^-$-induced endothelial injury as well as to the inhibition of reactive nitrogen and oxygen intermediates pro-inflammatory properties. In other words, we propose a positive feedback cycle in SCI. $ONOO^-$ decomposition catalyst would intercept this cycle at the level of NF-κB activation and cytokines release. This model would explain the reduction of cytokines formation and the inflammatory and immune cells infiltration during SCI in the ww-85-treated mice. In conclusion we have directly demonstrated that $ONOO^-$ is associated with the spinal cord damage evoked by trauma. The ww-85 may offer a novel approach for manipulating the pathological events that are associated with SCI. Just like with other porphyrins and antioxidants, additional redox properties of the ww-85 on other oxidant species (superoxide, hydrogen peroxide, nitroxyl anion, etc.) are possible. These additional actions may limit the specificity of the compound and may reduce its utility as a tool to dissect peroxynitrite-mediated pathogenetic processes from processes triggered by these above-mentioned oxidants. On the other hand, such additional actions may extend the therapeutic utility of these agents.

Further use of these catalysts as pharmacological tools in animal's models of human disease may lead us to a better understanding of when and where $ONOO^-$ plays a key role(s) in the development of inflammatory diseases such as SCI. This in turn should provide more effective treatment strategies for diseases in the clinic. In conclusion, $ONOO^-$ decomposition catalysts are not only useful tools for the pharmacological dissection of free radical-mediated pathology, but also offer promise as disease-modifying therapeutic agents capable of preserving the positive aspect of the double-edge sword of nitric oxide action.

***Declaration of interest*:** The authors report no conflicts of interest. The authors alone are responsible for the content and writing of the paper.

References

[1] Pineau I, Lacroix S. Proinflammatory cytokine synthesis in the injured mouse spinal cord: multiphasic expression pattern and identification of the cell types involved. J Comp Neurol 2007;500:267–285.

[2] Amar AP, Levy ML. Pathogenesis and pharmacological strategies for mitigating secondary damage in acute spinal cord injury. Neurosurgery 1999;44:1027–1040.

[3] Bao F, DeWitt DS, Prough DS, Liu D. Peroxynitrite generated in the rat spinal cord induces oxidation and nitration of proteins: Reduction by mn (iii) tetrakis (4-benzoic acid) porphyrin. J Neurosci Res 2003;71:220–227.

[4] Bao F, Liu D. Peroxynitrite generated in the rat spinal cord induces neuron death and neurological deficits. Neuroscience 2002;115:839–849.

[5] Bao F, Liu D. Peroxynitrite generated in the rat spinal cord induces apoptotic cell death and activates caspase-3. Neuroscience 2003;116:59–70.

[6] Liu D, Bao F, Prough DS, Dewitt DS. Peroxynitrite generated at the level produced by spinal cord injury induces peroxidation of membrane phospholipids in normal rat cord: reduction by a metalloporphyrin. J Neurotrauma 2005;22:1123–1133.

[7] Liu D, Ling X, Wen J, Liu J. The role of reactive nitrogen species in secondary spinal cord injury: formation of nitric oxide, peroxynitrite, and nitrated protein. J Neurochem 2000;75:2144–2154.

[8] Scott GS, Jakeman LB, Stokes BT, Szabo C. Peroxynitrite production and activation of poly (adenosine diphosphate-ribose) synthetase in spinal cord injury. Ann Neurol 1999;45:120–124.

[9] Scott GS, Szabo C, Hooper DC. Poly(adp-ribose) polymerase activity contributes to peroxynitrite-induced spinal cord neuronal cell death *in vitro*. J Neurotrauma 2004;21:1255–1263.

[10] Xiong Y, Rabchevsky AG, Hall ED. Role of peroxynitrite in secondary oxidative damage after spinal cord injury. J Neurochem 2007;100:639–649.

[11] Xu J, Kim GM, Chen S, Yan P, Ahmed SH, Ku G, Beckman JS, Xu XM, Hsu CY. Inos and nitrotyrosine expression after spinal cord injury. J Neurotrauma 2001;18:523–532.

[12] Bolanos JP, Heales SJ, Land JM, Clark JB. Effect of peroxynitrite on the mitochondrial respiratory chain: differential susceptibility of neurones and astrocytes in primary culture. J Neurochem 1995;64:1965–1972.

[13] Blanchard-Fillion B, Souza JM, Friel T, Jiang GC, Vrana K, Sharov V, Barron L, Schoneich C, Quijano C, Alvarez B, Radi R, Przedborski S, Fernando GS, Horwitz J, Ischiropoulos H. Nitration and inactivation of tyrosine hydroxylase by peroxynitrite. J Biol Chem 2001;276:46017–46023.
[14] Alvarez B, Radi R. Peroxynitrite reactivity with amino acids and proteins. Amino Acids 2003;25:295–311.
[15] Genovese T, Mazzon E, Muia C, Bramanti P, De Sarro A, Cuzzocrea S. Attenuation in the evolution of experimental spinal cord trauma by treatment with melatonin. J Pineal Res 2005;38:198–208.
[16] Salvemini D, Wang ZQ, Stern MK, Currie MG, Misko TP. Peroxynitrite decomposition catalysts: therapeutics for peroxynitrite-mediated pathology. Proc Natl Acad Sci USA 1998;95:2659–2663.
[17] Groves JT. Peroxynitrite: reactive, invasive and enigmatic. Curr Opin Chem Biol 1999;3:226–235.
[18] Misko TP, Highkin MK, Veenhuizen AW, Manning PT, Stern MK, Currie MG, Salvemini D. Characterization of the cytoprotective action of peroxynitrite decomposition catalysts. J Biol Chem 1998;273:15646–15653.
[19] Salvemini D, Jensen MP, Riley DP, Misko TP. Therapeutic manipulations of peroxynitrite. Drug News Perspect 1998; 11:204–214.
[20] Shimanovich R, Groves JT. Mechanisms of peroxynitrite decomposition catalyzed by fetmps, a bioactive sulfonated iron porphyrin. Arch Biochem Biophys 2001;387:307–317.
[21] Bianchi C, Wakiyama H, Faro R, Khan T, McCully JD, Levitsky S, Szabo C, Sellke FW. A novel peroxynitrite decomposer catalyst (fp-15) reduces myocardial infarct size in an in vivo peroxynitrite decomposer and acute ischemia-reperfusion in pigs. Ann Thorac Surg 2002;74: 1201–1207.
[22] Ferdinandy P, Danial H, Ambrus I, Rothery RA, Schulz R. Peroxynitrite is a major contributor to cytokine-induced myocardial contractile failure. Circ Res 2000;87:241–247.
[23] Pacher P, Liaudet L, Bai P, Mabley JG, Kaminski PM, Virag L, Deb A, Szabo E, Ungvari Z, Wolin MS, Groves JT, Szabo C. Potent metalloporphyrin peroxynitrite decomposition catalyst protects against the development of doxorubicin-induced cardiac dysfunction. Circulation 2003;107:896–904.
[24] Lancel S, Tissier S, Mordon S, Marechal X, Depontieu F, Scherpereel A, Chopin C, Neviere R. Peroxynitrite decomposition catalysts prevent myocardial dysfunction and inflammation in endotoxemic rats. J Am Coll Cardiol 2004;43:2348–2358.
[25] Genovese T, Mazzon E, Esposito E, Muia C, Di Paola R, Bramanti P, Cuzzocrea S. Beneficial effects of fetspp, a peroxynitrite decomposition catalyst, in a mouse model of spinal cord injury. Free Radic Biol Med 2007;43:763–780.
[26] Pieper GM, Nilakantan V, Chen M, Zhou J, Khanna AK, Henderson JD Jr, Johnson CP, Roza AM, Szabo C. Protective mechanisms of a metalloporphyrinic peroxynitrite decomposition catalyst, ww85, in rat cardiac transplants. J Pharmacol Exp Ther 2005;314:53–60.
[27] Mullane K. Neutrophil-platelet interactions and post-ischemic myocardial injury. Prog Clin Biol Res 1989;301: 39–51.
[28] Ohkawa H, Ohishi N, Yagi K. Assay for lipid peroxides in animal tissues by thiobarbituric acid reaction. Anal Biochem 1979;95:351–358.
[29] Sirin BH, Ortac R, Cerrahoglu M, Saribulbul O, Baltalarli A, Celebisoy N, Iskesen I, Rendeci O. Ischaemic preconditioning reduces spinal cord injury in transient ischaemia. Acta Cardiol 2002;57:279–285.
[30] Bethea JR, Castro M, Keane RW, Lee TT, Dietrich WD, Yezierski RP. Traumatic spinal cord injury induces nuclear factor-kappab activation. J Neurosci 1998;18:3251–3260.
[31] Basso DM, Beattie MS, Bresnahan JC. A sensitive and reliable locomotor rating scale for open field testing in rats. J Neurotrauma 1995;12:1–21.
[32] Joshi M, Fehlings MG. Development and characterization of a novel, graded model of clip compressive spinal cord injury in the mouse: Part 2. Quantitative neuroanatomical assessment and analysis of the relationships between axonal tracts, residual tissue, and locomotor recovery. J Neurotrauma 2002;19:191–203.
[33] Joshi M, Fehlings MG. Development and characterization of a novel, graded model of clip compressive spinal cord injury in the mouse: Part 1. Clip design, behavioral outcomes, and histopathology. J Neurotrauma 2002;19:175–90.
[34] Cuzzocrea S, Genovese T, Mazzon E, Crisafulli C, Min W, Di Paola R, Muia C, Li JH, Esposito E, Bramanti P, Xu W, Massuda E, Zhang J, Wang ZQ. Poly(adp-ribose) glycohydrolase activity mediates post-traumatic inflammatory reaction after experimental spinal cord trauma. J Pharmacol Exp Ther 2006;319:127–138.
[35] Genovese T, Mazzon E, Mariotto S, Menegazzi M, Cardali S, Conti A, Suzuki H, Bramanti P, Cuzzocrea S. Modulation of nitric oxide homeostasis in a mouse model of spinal cord injury. J Neurosurg Spine 2006;4:145–153.
[36] Glaser J, Gonzalez R, Sadr E, Keirstead HS. Neutralization of the chemokine cxcl10 reduces apoptosis and increases axon sprouting after spinal cord injury. J Neurosci Res 2006;84:724–734.
[37] Tator CH. Review of experimental spinal cord injury with emphasis on the local and systemic circulatory effects. Neurochirurgie 1991;37:291–302.
[38] Anderson DK, Hall ED. Pathophysiology of spinal cord trauma. Ann Emerg Med 1993;22:987–992.
[39] Radi R, Beckman JS, Bush KM, Freeman BA. Peroxynitrite-induced membrane lipid peroxidation: the cytotoxic potential of superoxide and nitric oxide. Arch Biochem Biophys 1991;288:481–487.
[40] Klebanoff SJ. Reactive nitrogen intermediates and antimicrobial activity: role of nitrite. Free Radic Biol Med 1993;14:351–360.
[41] Bohle DS. Pathophysiological chemistry of nitric oxide and its oxygenation by-products. Curr Opin Chem Biol 1998;2:194–200.
[42] Greenacre SA, Ischiropoulos H. Tyrosine nitration: localisation, quantification, consequences for protein function and signal transduction. Free Radic Res 2001;34:541–581.
[43] Cuzzocrea S, Riley DP, Caputi AP, Salvemini D. Antioxidant therapy: a new pharmacological approach in shock, inflammation, and ischemia/reperfusion injury. Pharmacol Rev 2001;53:135–159.
[44] Pasternack RF, Gillies BS, Stromsted JP. Substitution reactions of a water-soluble metalloporphyrin with azide and 1,1,3,3-tetramethyl-2-thiourea. Bioinorg Chem 1978;8: 33–44.
[45] Balavoine GG, Geletti YV, Bejan D. Catalysis of peroxynitrite reactions by manganese and iron porphyrins. Nitric Oxide 1997;1:507–521.
[46] Szabo C, Mabley JG, Moeller SM, Shimanovich R, Pacher P, Virag L, Soriano FG, Van Duzer JH, Williams W, Salzman AL, Groves JT. Part i: Pathogenetic role of peroxynitrite in the development of diabetes and diabetic vascular complications: studies with fp15, a novel potent peroxynitrite decomposition catalyst. Mol Med 2002;8:571–580.
[47] Digerness SB, Harris KD, Kirklin JW, Urthaler F, Viera L, Beckman JS, Darley-Usmar V. Peroxynitrite irreversibly decreases diastolic and systolic function in cardiac muscle. Free Radic Biol Med 1999;27:1386–1392.
[48] Mabley JG, Suarez-Pinzon WL, Hasko G, Salzman AL, Rabinovitch A, Kun E, Szabo C. Inhibition of poly (adp-ribose) synthetase by gene disruption or inhibition with

5-iodo-6-amino-1,2-benzopyrone protects mice from multiple-low-dose-streptozotocin-induced diabetes. Br J Pharmacol 2001;133:909–919.

[49] Maybauer DM, Maybauer MO, Szabo C, Westphal M, Traber LD, Enkhbaatar P, Murthy KG, Nakano Y, Salzman AL, Herndon DN, Traber DL. Lung-protective effects of the metalloporphyrinic peroxynitrite decomposition catalyst ww-85 in interleukin-2 induced toxicity. Biochem Biophys Res Commun 2008;377:786–791.

[50] Beckman JS, Koppenol WH. Nitric oxide, superoxide, and peroxynitrite: the good, the bad, and ugly. Am J Physiol 1996;271:C1424–C1437.

[51] Eiserich JP, Hristova M, Cross CE, Jones AD, Freeman BA, Halliwell B, van der Vliet A. Formation of nitric oxide-derived inflammatory oxidants by myeloperoxidase in neutrophils. Nature 1998;391:393–397.

[52] Sampson JB, Ye Y, Rosen H, Beckman JS. Myeloperoxidase and horseradish peroxidase catalyze tyrosine nitration in proteins from nitrite and hydrogen peroxide. Arch Biochem Biophys 1998;356:207–213.

[53] Naidu BV, Fraga C, Salzman AL, Szabo C, Verrier ED, Mulligan MS. Critical role of reactive nitrogen species in lung ischemia-reperfusion injury. J Heart Lung Transplant 2003;22:784–793.

[54] Bowie A, O'Neill LA. Oxidative stress and nuclear factor-kappab activation: a reassessment of the evidence in the light of recent discoveries. Biochem Pharmacol 2000;59:13–23.

[55] Haddad JJ. Antioxidant and prooxidant mechanisms in the regulation of redox(y)-sensitive transcription factors. Cell Signal 2002;14:879–897.

[56] Verma IM. Nuclear factor (nf)-kappab proteins: therapeutic targets. Ann Rheum Dis 2004;63(Suppl 2):ii57–ii61.

[57] Genovese T, Mazzon E, Crisafulli C, Di Paola R, Muia C, Bramanti P, Cuzzocrea S. Immunomodulatory effects of etanercept in an experimental model of spinal cord injury. J Pharmacol Exp Ther 2006;316:1006–1016.

[58] Streit WJ, Semple-Rowland SL, Hurley SD, Miller RC, Popovich PG, Stokes BT. Cytokine mrna profiles in contused spinal cord and axotomized facial nucleus suggest a beneficial role for inflammation and gliosis. Exp Neurol 1998;152:74–87.

[59] Liu J, Marino MW, Wong G, Grail D, Dunn A, Bettadapura J, Slavin AJ, Old L, Bernard CC. Tnf is a potent anti-inflammatory cytokine in autoimmune-mediated demyelination. Nat Med 1998;4:78–83.

[60] Ousman SS, David S. Mip-1alpha, mcp-1, gm-csf, and tnf-alpha control the immune cell response that mediates rapid phagocytosis of myelin from the adult mouse spinal cord. J Neurosci 2001;21:4649–4656.

[61] Shafit-Zagardo B, Sharma N, Berman JW, Bornstein MB, Brosnan CF. Csf-1 expression is upregulated in astrocyte cultures by il-1 and tnf and affects microglial proliferation and morphology in organotypic cultures. Int J Dev Neurosci 1993;11:189–198.

[62] Sharma HS, Winkler T, Stalberg E, Gordh T, Alm P, Westman J. Topical application of tnf-alpha antiserum attenuates spinal cord trauma induced edema formation, microvascular permeability disturbances and cell injury in the rat. Acta Neurochir Suppl 2003;86:407–413.

[63] Genovese T, Mazzon E, Rossi A, Di Paola R, Cannavo G, Muia C, Crisafulli C, Bramanti P, Sautebin L, Cuzzocrea S. Involvement of 5-lipoxygenase in spinal cord injury. J Neuroimmunol 2005;166:55–64.

[64] Crocker SJ, Whitmire JK, Frausto RF, Chertboonmuang P, Soloway PD, Whitton JL, Campbell IL. Persistent macrophage/microglial activation and myelin disruption after experimental autoimmune encephalomyelitis in tissue inhibitor of metalloproteinase-1-deficient mice. Am J Pathol 2006;169:2104–2116.

[65] Holtz A, Nystrom B, Gerdin B. Spinal cord injury in rats: inability of nimodipine or anti-neutrophil serum to improve spinal cord blood flow or neurologic status. Acta Neurol Scand 1989;79:460–467.

[66] Fan LH, Wang KZ, Cheng B, Wang CS, Dang XQ. Anti-apoptotic and neuroprotective effects of tetramethylpyrazine following spinal cord ischemia in rabbits. BMC Neurosci 2006;7:48.

[67] Scholz J, Broom DC, Youn DH, Mills CD, Kohno T, Suter MR, Moore KA, Decosterd I, Coggeshall RE, Woolf CJ. Blocking caspase activity prevents transsynaptic neuronal apoptosis and the loss of inhibition in lamina ii of the dorsal horn after peripheral nerve injury. J Neurosci 2005;25:7317–7323.

[68] Woodhouse A, Vincent AJ, Kozel MA, Chung RS, Waite PM, Vickers JC, West AK, Chuah MI. Spinal cord tissue affects ensheathing cell proliferation and apoptosis. Neuroreport 2005;16:737–740.

[69] Merrill JE, Ignarro LJ, Sherman MP, Melinek J, Lane TE. Microglial cell cytotoxicity of oligodendrocytes is mediated through nitric oxide. J Immunol 1993;151:2132–2141.

[70] Wang JY, Shum AY, Ho YJ, Wang JY. Oxidative neurotoxicity in rat cerebral cortex neurons: Synergistic effects of h2o2 and no on apoptosis involving activation of p38 mitogen-activated protein kinase and caspase-3. J Neurosci Res 2003;72:508–519.

[71] Chittenden T, Harrington EA, O'Connor R, Flemington C, Lutz RJ, Evan GI, Guild BC. Induction of apoptosis by the bcl-2 homologue bak. Nature 1995;374:733–736.

[72] Bar-Peled O, Knudson M, Korsmeyer SJ, Rothstein JD. Motor neuron degeneration is attenuated in bax-deficient neurons *in vitro*. J Neurosci Res 1999;55:542–556.

[73] Pieper AA, Verma A, Zhang J, Snyder SH. Poly (adp-ribose) polymerase, nitric oxide and cell death. Trends Pharmacol Sci 1999;20:171–181.

[74] LaPlaca MC, Raghupathi R, Verma A, Pieper AA, Saatman KE, Snyder SH, McIntosh TK. Temporal patterns of poly(adp-ribose) polymerase activation in the cortex following experimental brain injury in the rat. J Neurochem 1999;73:205–213.

This paper was first published online on iFirst on 2 May 2009.